AIAA JOURNAL
Vol. 36, No. 5, May 1998

Residual Strength of Aging Aircraft with Multiple Site Damage/Multiple Element Damage

L. Wang*
University of California, Los Angeles, Los Angeles, California 90095
and
W. T. Chow,† H. Kawai,† and S. N. Atluri‡
Georgia Institute of Technology, Atlanta, Georgia 30332-0356

A numerical study is presented of the residual strength of an aircraft fuselage in the presence of multiple site damage (MSD)/multiple element damage. The analyses were carried out using a software package that was developed to facilitate automated analyses of full-scale fuselage panels with widespread fatigue damage, using a hierarchical approach and elastic–plastic finite element alternating method. The present study shows the importance of elastic–plastic fracture mechanics in the assessment of the residual strength of a fuselage with two-bay longitudinal/circumferential lead cracks, with and without MSD, and of the interaction between multiple lead cracks.

I. Introduction

STRUCTURAL integrity evaluation of aging aircraft structures is extremely important in ensuring their continued airworthiness. A fuselage of a commercial aircraft typically undergoes a cycle of pressurization for every single flight operation. These cycles of pressurization would result in fatigue cracking near the rivet holes of the fuselage panel and could lead to a widespread fatigue damage (WFD) situation. With the formation of WFD in the fuselage panel, the fuselage structure may no longer meet the damage tolerance requirement.

Recent studies suggest that WFD can significantly reduce the residual strength of an aircraft fuselage.[1–8] Damage tolerance requires that a fuselage be designed so as to prevent a two-bay crack, in either the longitudinal or circumferential direction (as shown in Fig. 1), from unstable crack propagation. This requirement is to ensure the ability of the structure to sustain discrete source damage induced by a foreign object. Under the current damage tolerance philosophy, the inspection program of a fuselage panel is established on the basis that a single lead crack, propagating between detectable and critical size at limit load, will be detected before failure. This single lead crack is intended to represent a discrete source damage from fatigue, accident, or corrosion in service. However, when widespread fatigue damage exists in the fuselage panel, the interaction of the lead crack with WFD has to be studied, and the damage tolerance requirement of this structure needs to be changed accordingly to ensure that the structure with WFD would meet the same safety requirements of a structure without WFD. Some preliminary analyses performed by Swift,[3] based on two-dimensional solutions, have shown that the residual strength of a fuselage can be degraded below the required levels when small cracks (with size of the order 0.05 in.) exist ahead of the lead crack. Furthermore, based on experiments on flat panels, Maclin[2] has found that cracks as small as 0.05 in. ahead of the lead crack can reduce the residual strength by more than 30%. To ensure the airworthiness of aging structures, a study of the interaction between MSD cracks and a two-bay crack is necessary to determine whether the residual strength of the fuselage panel is reduced to below the required level.

Received March 10, 1997; revision received Oct. 29, 1997; accepted for publication Oct. 30, 1997.

*Postdoctoral Fellow, Center for Aerospace Research and Education.
†Postdoctoral Fellow, Computational Modeling Center.
‡Institute Professor, Regents' Professor of Engineering, Hightower Chair in Engineering, and Director, Computational Modeling Center; currently Director, Center for Aerospace Research and Education, 7704 Boelter Hall, School of Engineering and Applied Science, University of California, Los Angeles, Los Angeles, CA 90024. Fellow AIAA.

Given that the cost of computing has declined by several orders of magnitude over the past decade, it is now economically feasible to perform numerical analysis of a full-scale pressurized fuselage panel to study not just a single two-bay crack but also the interactions of multiple cracks (for example, due to multiple engine fragments) in stiffened structures. Therefore, the interaction between multiple lead cracks, to simulate discrete source damage induced by fragments in the event of an engine disintegration, is also studied in this paper. Furthermore, it is also possible to include certain nonlinear features, such as the elastic–plastic material behavior, to accurately calculate the interactions of plastic zones. With the ability to model a full-scale fuselage panel with computational ease, the effect of location of the two-bay crack, either in the longitudinal direction or in the circumferential direction, is pursued.

A software package has been developed to facilitate automated analysis of full-scale fuselage panels with WFD. After a brief description of the software package, this paper presents a numerical study, carried out using this software package, of the residual strength of an aircraft fuselage in the presence of multiple site damage (MSD)/multiple element damage (MED). The importance of elastic–plastic fracture mechanics (EPFM) in the assessment of the residual strength of a fuselage with longitudinal/circumferential lead cracks, and with and without MSD, is discussed. Also, the effects of interaction between multiple lead cracks are presented and discussed.

II. Automated Evaluation of Residual Strength in the Presence of WFD

A software package with a user-friendly graphical user interface (GUI) has been developed to efficiently perform the fatigue/fracture analysis of MSD in fuselages with various designs of frames and stiffeners. To substantially reduce the cost of computing, the global/intermediate/local hierarchical modeling approach is used. The software automatically generates the finite element mesh of the skins, stiffeners, frames, and rivets for each level of modeling, using the data provided through the GUI interface. It also extracts automatically the boundary conditions for the intermediate/local models from the results of global/intermediate analyses, respectively. The global and intermediate analyses are carried out using a standard finite element method, wherein the cracks are modeled explicitly with a coarse mesh, to obtain the load flow pattern around the damage zone near the MSD cracks. A local analysis, based on the elastic–plastic finite element alternating method (EPFEAM),[6–8] follows the global/intermediate analyses to obtain the elastic–plastic fracture parameters[1,9,10] (the J integral or the T^* integral). There is no need to model the cracks explicitly in the local analysis because the EPFEAM is used. At the end of the analysis, the software provides the graphical output of the residual life and strength estimates

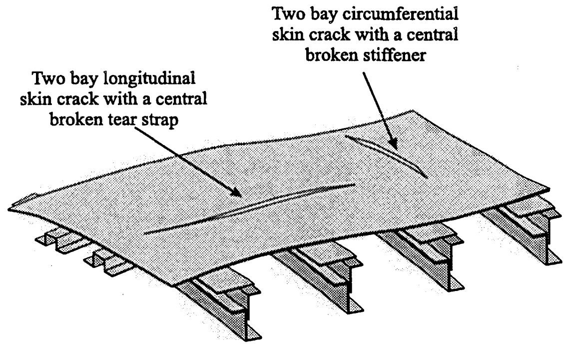

Fig. 1 Damage tolerance requirement based on a two-bay crack.

for the fuselage with MSD in the presence of a discrete source damage.

In the global analysis, conventional linear elastic finite element analysis of the multibay stiffened shell panel is performed. The fuselage skin is modeled by eight noded shell elements with five degrees of freedom per node, whereas the frame, stringer, and tear strap are modeled by three noded beam elements. The fasteners in the fuselage panel are modeled by using spring elements and multiple point constraints. The stiffness of the fastener, when it is assumed to behave linear elastically in the global model, is represented by the empirical relation[11]

$$K_F = \frac{ED}{A + C(D/t_1) + (D/t_2)} \tag{1}$$

with $A = 5.0$ and $C = 0.8$ for aluminum rivets. D and E are the diameter and elastic modulus of the rivet, respectively, and t is the thickness of the skin. Whenever there is a crack, the stiffness of the fasteners along the crack length becomes zero as the fasteners will not be able to bear load in that direction. A typical global model, shown in Fig. 2a, has 7 frames and 20 stringers with approximately 3000 elements.

After the global analysis, which uses a coarse mesh to capture the overall load flow of a large section of a fuselage panel, the displacement boundary conditions of a smaller section are transferred to an intermediate model. This intermediate model contains the entire lead crack of the fuselage panel. In the intermediate analysis, the frames, stringers, and fasteners are modeled in greater detail; each of the fasteners is properly positioned according to the physical model, whereas the frames and the stringers are modeled with four noded shell elements, as shown in Fig. 2b. In this intermediate analysis, the capability of analyzing nonlinear fastener behavior as well as nonlinear geometric behavior is provided. To capture the interaction between the lead crack with much smaller MSD cracks, a local analysis of a smaller section of the fuselage skin is carried out. In the local model, the rivet loads are distributed on the rivet hole periphery according to an analytical solution; no separate elastic–plastic contact analysis of the rivet with the hole is performed. Such contact analyses are presently underway. The rivet holes are meshed in detail, as shown in Fig. 2c, and the elastic–plastic material behavior is accounted for.

It is assumed that the details of the fuselage panel are provided by the original equipment manufacturer or can be easily obtained from a database. A user can choose the orientation of the cracks in either the longitudinal or circumferential direction. The center of the lead crack, with respect to the frame/stringer position, can be changed to study the effect of crack location on the residual strength of the fuselage panel. To obtain the residual strength curve, the user would be asked to input the initial and final crack lengths. For a longitudinal crack, the user is also given an option on whether the tear strap is broken, and for a circumferential crack, the user is given an option on whether the stringer is broken. After the interactive input session, the program automatically generates the appropriate global/intermediate/local models for the analyses.

III. Two-Bay Crack in the Longitudinal Direction

The fuselage shell panel under consideration is a typical wide-body commercial aircraft. It is stiffened along the longitudinal

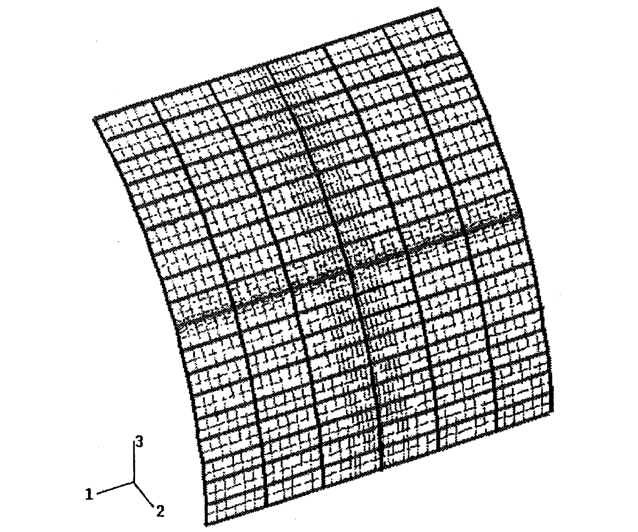

a) Global model

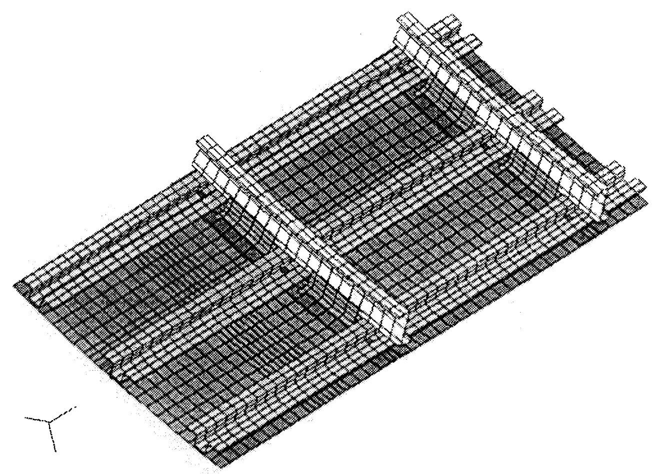

b) Intermediate model

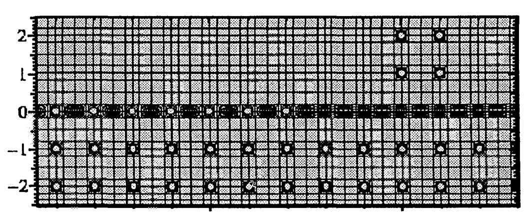

c) Local model

Fig. 2 Global/intermediate/local hierarchical process.

direction by stringers and in the circumferential direction by frames and tear straps. The tear strap at the center of the two-bay crack is assumed to be broken. The skins, frames, stringer, and rivets are assumed to be made of aluminum, whereas the tear strap is made of titanium. The overall dimensions of the fuselage are given in Fig. 3. The critical stress intensity factor for the aluminum skin is taken to be 90 ksi$\sqrt{\text{in}}$. For the elastic–plastic analysis, the T^* (with an equivalent critical value of 0.771 ksi · in.) integral (see Refs. 1 and 6–9 for further details) is used as the fracture criterion.

Earlier, in Refs. 1 and 6–8, a detailed discussion of the residual strength of flat unstiffened panels with lead cracks, in the presence of MSD, has been presented. In these studies, detailed residual strength calculations based on linear elastic fracture mechanics (LEFM) as well as EPFM were presented. Also, detailed comparisons with test data for 10 different panels, based on tests conducted at the National Institute of Standards and Technology, were performed.[6–8] Based on these studies,[1,6–8] it has been established that the predictions of residual strength in the presence of MSD agreed extremely well with test data when EPFM was used, whereas similar predictions were anticonservative, i.e., the predictions of residual strength were

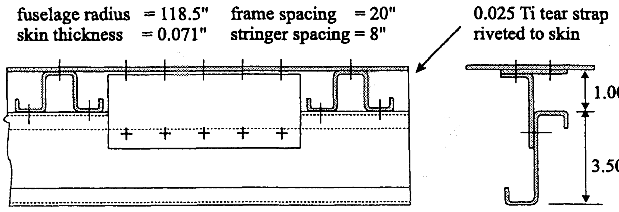

Fig. 3 Geometric dimensions of the fuselage panel.

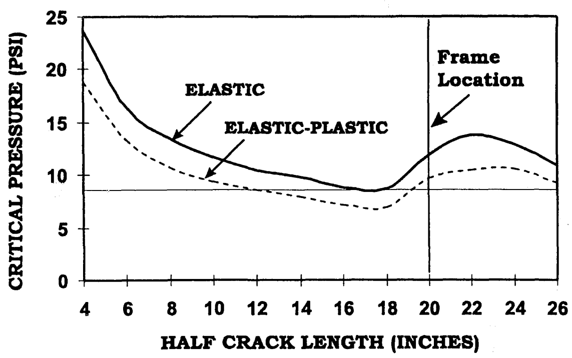

Fig. 4 Residual strength as a function of the crack size.

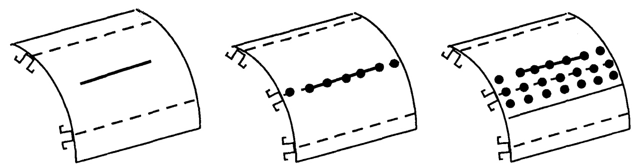

a) In between two stringers b) On a stringer c) On a lapjoint

Fig. 5 Locations of the two-bay crack.

much higher than the test data, when LEFM was used. In extending the results of Refs. 6–8, the present paper considers the residual strength of a built-up stiffened curved fuselage panel with a lead crack and MSD.

In this study, the residual strength of the fuselage panel has been calculated as a function of the lead crack size. In Fig. 4, the horizontal line (at 8.6 psi) represents the typical operating internal pressure in a fuselage of a commercial plane. The solid curve represents, for each length of the lead crack, the pressure at which the lead crack would become unstable, as predicted by LEFM, i.e., the pressure at which the computed K factor becomes equal to the fracture toughness. Thus, the residual strength for different lengths of the lead crack, as predicted by LEFM, is the vertical distance between the solid curve and the horizontal line represented by 8.6 psi. Likewise, the vertical distance between the broken curve and the horizontal line represented by 8.6 psi is the residual strength for different lengths of the lead crack, as predicted by EPFM. Thus, it is seen that the predictions based on LEFM are anticonservative (thus giving a false sense of security) as compared with those based on EPFM.

A two-bay crack has been placed at three different locations to examine the effect that the location of the two-bay crack would have on the overall residual strength curve, as shown in Fig. 5. In Fig. 5a, the two-bay crack lies in the middle of two stringers; in Fig. 5b, the two-bay crack lies in the row of fasteners on the top of a stringer; and finally in Fig. 5c, the two-bay crack lies on the top of the fastener row of the upper skin section of a lapjoint. It has been found that the residual strength of a two-bay crack for the case of Fig. 5a is significantly higher than that of the cases of Figs. 5b and 5c, as shown in Fig. 6. Furthermore, assuming that the operating pressure in the fuselage is 8.6 psi, Fig. 6 shows that a two-bay crack for the case of Fig. 5a would be arrested ahead of the frame, whereas the two-bay crack for the case of Fig. 5b would not be arrested until the crack tip passes the frame location. The differences in the residual strength for these three locations can be attributed to the design of the frames. As can be seen from Fig. 7, when the crack lies between two stringers, there is an additional frame clip that constrains the two-bay crack

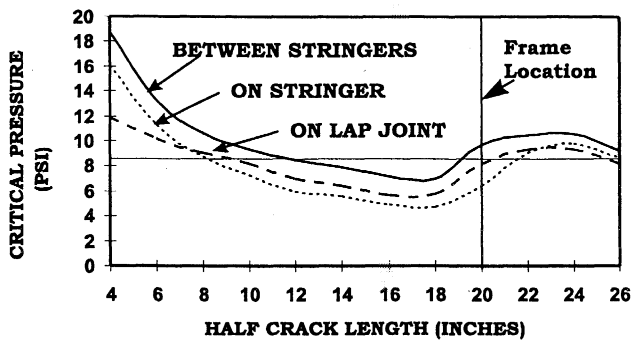

Fig. 6 Residual strength curve for a two-bay crack at different locations.

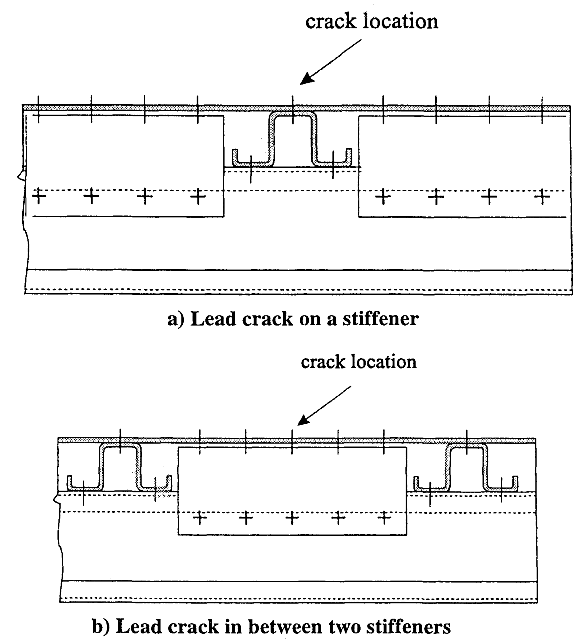

Fig. 7 Effect of frame design on the residual strength of a two-bay crack.

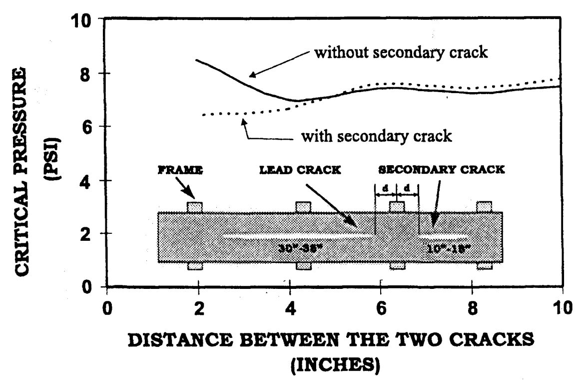

Fig. 8 Interaction between two large cracks.

from opening. However, when the crack lies on the stringer or on the lapjoint, there is no secondary frame to constrain the crack from opening.

IV. Interaction Between Multiple Cracks

First, consider the interaction between a two-bay crack and a single-bay crack. Both of these cracks lie in the middle, between two stringers. The center of the two-bay crack would lie on the frame, whereas the center of the single-bay crack would lie in the middle of the bay. The sizes of these two cracks are varied such that both crack tips have an equal distance d to the frame position, as shown in Fig. 8. (Note that Fig. 8 shows only the local model in the earlier described hierarchical modeling of the curved stiffened fuselage.)

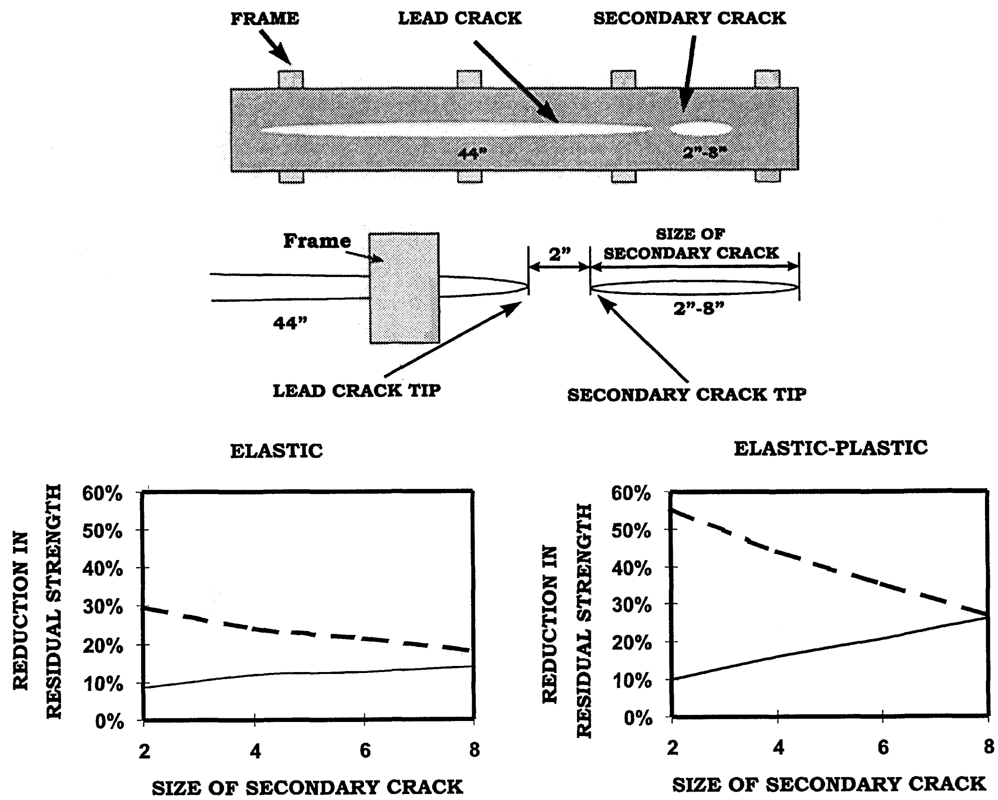

Fig. 9 Interaction between a lead crack and a secondary crack: ——, lead crack tip, and – – –, secondary crack tip.

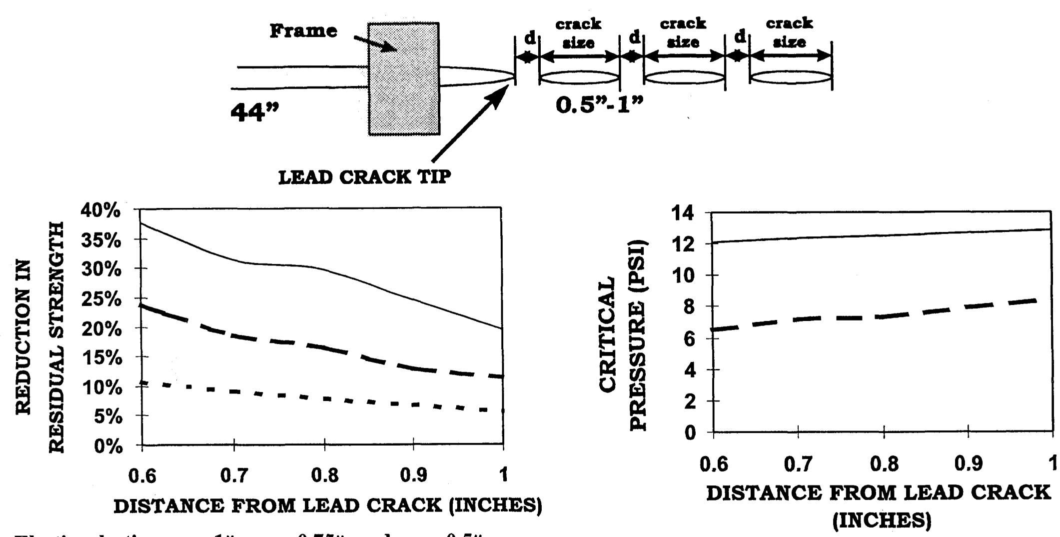

Elastic–plastic: ——, 1″; – – –, 0.75″; and - - - -, 0.5″

Residual strength curve for 1″ crack: ——, elastic, and – – –, elastic–plastic

Fig. 10 Interaction of a lead crack with three smaller cracks.

The result from Fig. 8 shows little interaction between these two cracks when the distance between the two crack tips is more than 4 in., even though the size of the lead crack may be as large as 36 in. However, when these two crack tips are only 2 in. apart, the residual strength of the fuselage panel is reduced by more than 20%. The strong interactions between these two cracks can be attributed to the plastic zones for the two crack tips interacting with each other.

As shown in Fig. 4, the maximum arresting capability of the stiffener occurs when the size of the two-bay crack exceeds the two-frame interval. Therefore, to understand how a secondary crack can reduce the maximum arresting capability of the stiffener, the size of the lead crack in this example is chosen to exceed the two-frame interval by 4 in. In this example, the secondary crack is 2 in. ahead of the lead crack and the size of the secondary crack is varied from 2 to 8 in., as shown in Fig. 9. The result shows that the reduction of critical pressure in the presence of the lead crack varies linearly with the size of the secondary crack, from 10 to 30% (based on elastic–plastic analysis). Furthermore, the result also shows that the larger lead crack has more influence on the smaller secondary crack than the smaller secondary crack would have on the lead crack. A comparison between linear elastic and elastic–plastic analysis shows that the linear elastic solution would significantly underestimate the severity of the interaction between these two cracks.

In the next example, the extent of the reduction in residual strength, due to three smaller cracks in front of the two-bay crack, is studied. The elastic–plastic analysis shows that the residual strength of the lead crack is influenced not only by the size of the smaller cracks but more importantly by the distance of these cracks from the lead crack, as shown in Fig. 10. Furthermore, it has been found that, when the same analyses for the 1-in. cracks are performed using the linear elastic assumption, the residual strength would be overestimated by a factor of two. Similar studies were also carried out to examine the effect of the interactions of MSD cracks with the two-bay crack. The result given in Fig. 11 shows that the residual strength of the lead crack would be reduced by 10% when the size of the MSD cracks is 0.2 in. Again, as seen in Fig. 11, the linear elastic assumption greatly underestimates the interaction between the lead crack and the MSD cracks.

V. Two-Bay Cracks in the Circumferential Direction

Much research has been devoted to the studies of cracks in the fuselage lap joints. However, circumferential cracks may result in more serious consequences if their growth cannot be arrested by the stiffened structure of an aircraft fuselage. Circumferential cracks received less attention because the axial stress due to pressurization is smaller than the hoop stress caused by pressurization. However, the axial skin stress at certain locations on the aircraft fuselage, as illustrated in Fig. 12, can be higher than the hoop stress, due to the fuselage down bending and the cabin pressure. The axial stress can be as high as 34 ksi (see Ref. 5), which is about 70% of the initial yield stress. (The initial yield stress of AL 2024-T3 is 47 ksi.) Because the panel works at such a high level of gross stress, even a small stress concentration factor can lead to yielding. Therefore, extensive plastic deformation can be expected in the presence of a lead crack, and nonlinear material behavior becomes very important in the study of residual strength in such a case.

The following is a brief description of the panel under consideration. The location of a circumferential crack in a component test is shown in Fig. 13. More details may be found in Ref. 11. The skin is AL 2024-T3 and 0.071 in. thick. Stringer spacing is 8 in. The cross-sectional area of each stringer is 0.5471 in.^{2} In the test the panel failed at the gross stress of 39.7 ksi, with the half-crack length equal to 9.88 in. The fracture toughness of the skin material is 198 ksi$\sqrt{\text{in.}}$, as suggested by Swift.[5]

Figure 14 shows the residual strength curves obtained using LEFM and EPFM. When the computed residual strength is compared to the load at the failure as determined in a test,[11] it is seen that the LEFM prediction overestimates the residual strength of the panel by a large amount. However, the EPFM approach only slightly underestimated the residual strength of the panel. Here, the residual strength curve is obtained by computing the failure load at different crack sizes. Therefore, the effect of stable tearing of the skin is not considered. In the test,[11] a static loading was applied on the panel to force the crack to grow from a half-crack length of 7.38 in. to the final failure. Because of the plastic hardening, the panel can take slightly higher load than at the crack initiation. Therefore, the load at crack initiation will be slightly smaller than the failure load observed in the test. Thus, we consider the prediction obtained by the EPFM approach to be very good.

Figure 15 shows the equivalent plastic strain contour plots for cracks of different sizes at the critical loads. It is seen that the plastic zones are very large, with a radius of more than 5 in. The plastic deformations around the rivet holes can also be recognized by the small dark zones near the locations of the rivet holes. As the crack size increases, the center broken stringer takes a smaller load. This is indicated by the disappearance of plastic deformations near the rivet holes located at the center stringer. More and more load is transferred onto the crack-arresting stringers as the crack size increases, as indicated by the plastic deformations near the rivet

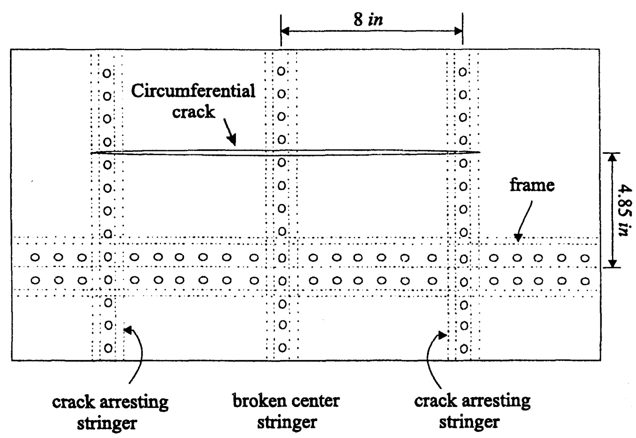

Fig. 13 Location of a circumferential crack in a component test.

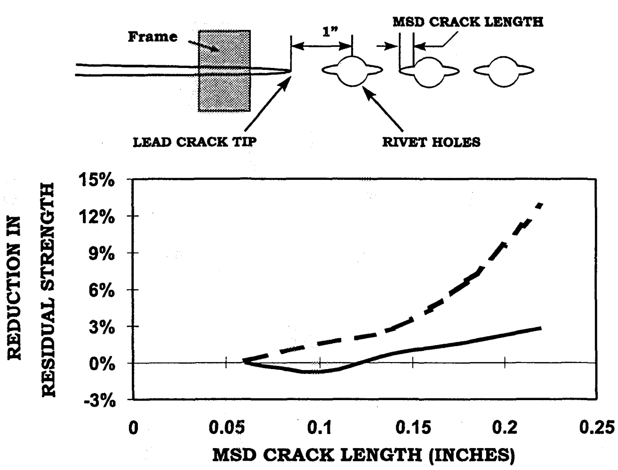

Fig. 11 Interaction of a lead crack with MSD cracks: ——, elastic, and – – –, elastic–plastic.

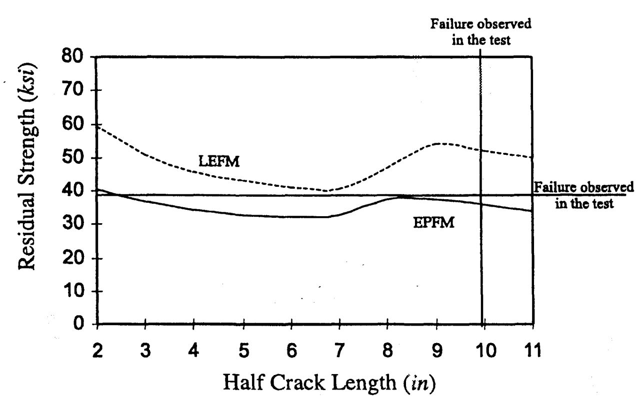

Fig. 14 Residual strength curve for the circumferential crack.

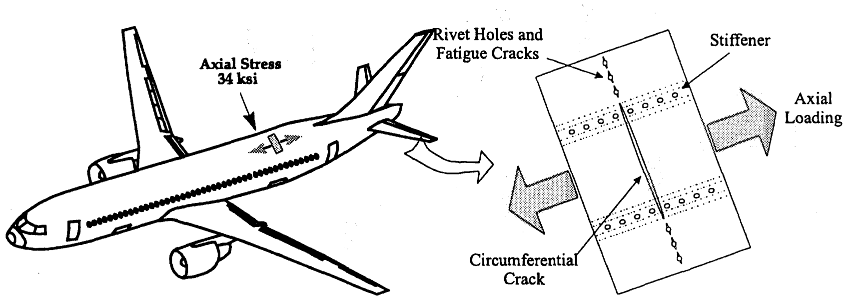

Fig. 12 Critical location on the aircraft fuselage for circumferential cracks.

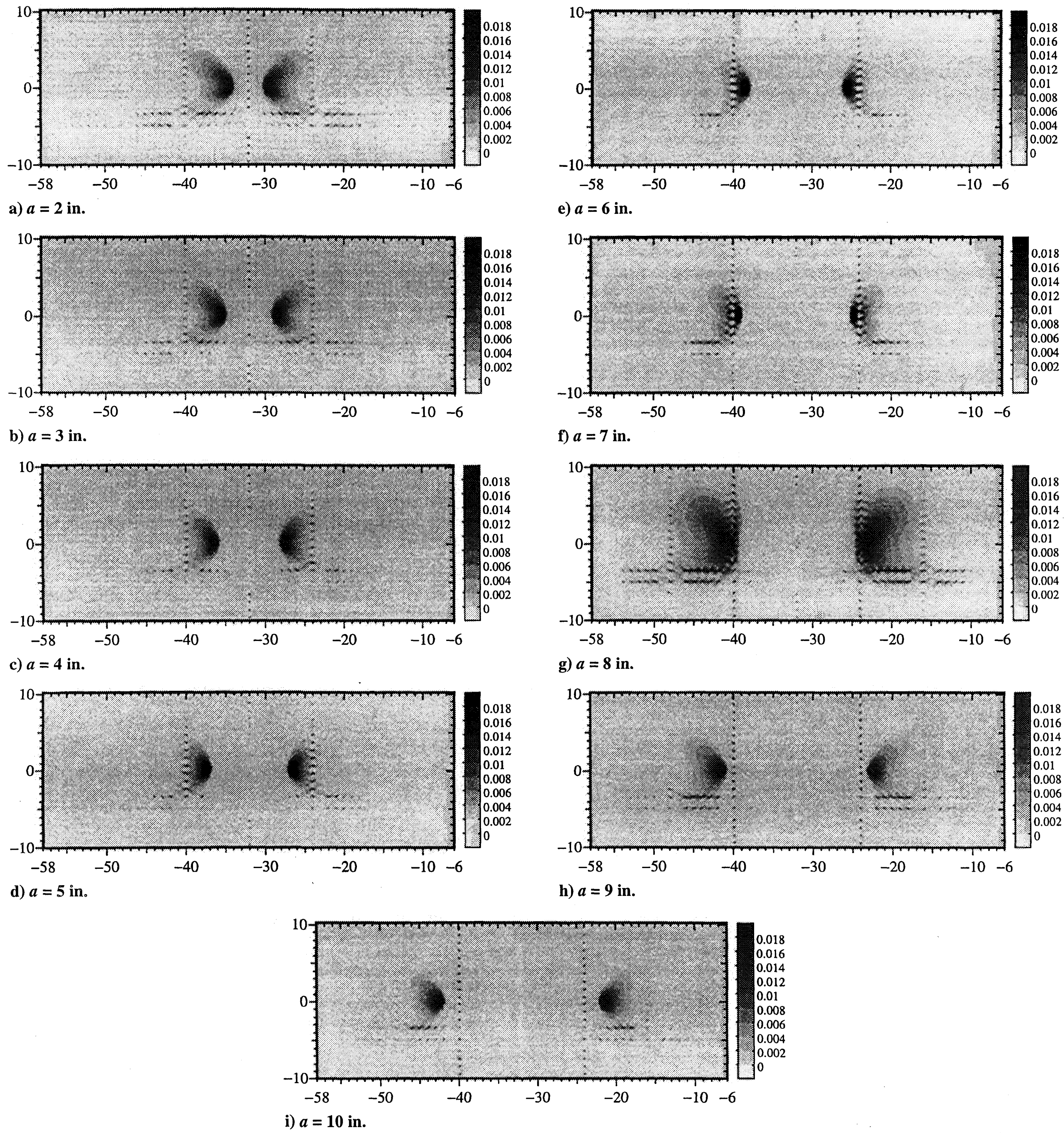

Fig. 15 Equivalent plastic strain contour plots for lead cracks of different half-lengths.

holes at the crack-arresting stringers. As the crack tips approach the crack-arresting stringer, the plastic deformations around the crack tips are restricted by the stringers. However, right after the crack tips penetrate the crack-arresting stringers, as seen in the contour plot, Fig. 15g ($a = 8$ in.), the size of plastic deformation reaches the maximum. At this point, the residual strength curve reaches a local maximum point (see Fig. 14), and the crack-arresting stringers are behind the crack tips.

The plastic deformations are nearly symmetric about the crack plane for all crack sizes, though they are disturbed near the location of the frame (located below the crack in the contour plots). This indicates that the effect of the frame is not significant.

Figure 16 shows the residual strength curves for the circumferentially cracked panel with frames of different size. In this analysis, we doubled the size of the frame to study the effect of the frame. It is seen that the size of the frame almost makes no difference. In a real structure, the skin of the fuselage will buckle in the presence of a large crack. A frame near the crack can act as an antibuckling guide. In this hierarchical analysis, no buckling is allowed. Therefore, the antibuckling effect of the frame is not studied.

Figure 17 shows the effect of cabin pressurization. In Fig. 17, we compute the residual strength for the case where there is only axial loading and for the case where there are both axial loading and hoop stress (due to pressurization). Because the pressurization changes mainly the hoop stress, which does not affect mode-I loading of the circumferential crack, little difference in the residual strength curves is observed in both the linear elastic fracture analysis and the elastic–plastic fracture analysis.

In the test,[11] it was observed that the panel failure was precipitated by rivet failure in the crack-arresting stringers. Because the rivets on the crack-arresting stringers transfer the load from the skin to the stringers, the nonlinear behavior of the rivets can have a considerable

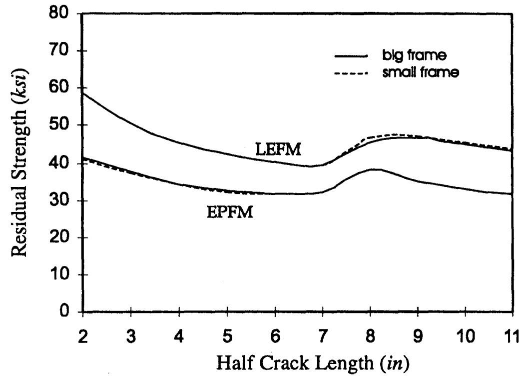

Fig. 16 Residual strength curves for the circumferentially cracked panel with frames of different sizes.

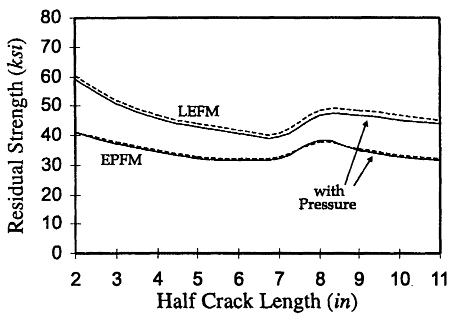

Fig. 17 Residual strength curves for the circumferentially cracked panel with and without cabin pressure.

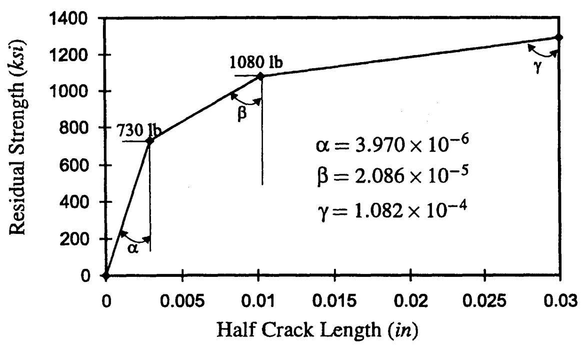

Fig. 18 Nonlinear rivet-flexibility curve.

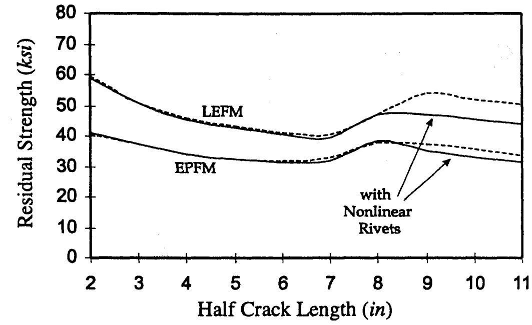

Fig. 19 Effect of the nonlinear behavior of rivets.

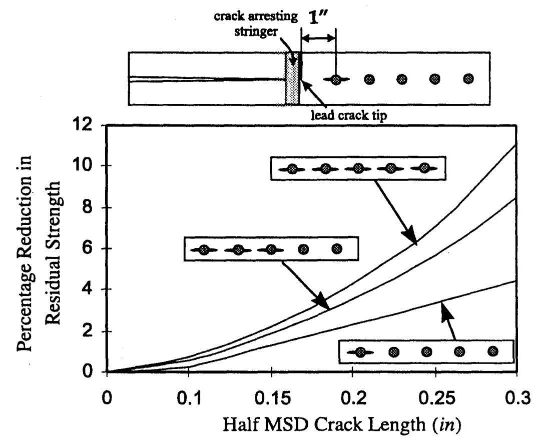

Fig. 20 Percentage reduction in the residual strength due to MSD cracks.

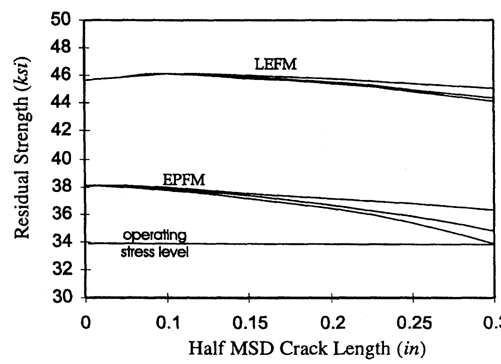

Fig. 21 Residual strength in the presence of MSD cracks and a lead crack with a half-crack length of 8 in.

effect on the crack-arresting capability of the panel. To study this effect, we use the empirical flexibility curve[5] to model the nonlinear effect of the rivets on the residual strength of the panel. The empirical flexibility curve is shown in Fig. 18. This flexibility curve was obtained from an experiment in which a riveted joint was loaded until the rivet failed.[5] Therefore, this flexibility curve includes the actual plastic deformation of the skin.

The effect of nonlinear behavior of rivets can be seen in Fig. 19. Because of the yielding of rivets, a smaller load is transferred onto the stringer from the skin. This decreases the residual strength of the cracked panel. The reduction is observed in both the LEFM analysis and the EPFM analysis. However, the influence of the nonlinear behavior of rivets is smaller in the EPFM analysis because the yielding of the skin around rivet holes was modeled in the EPFM analysis.

Multiple site fatigue damages can reduce the residual strength of an aircraft fuselage in the presence of a large circumferential crack. Figure 20 shows the percentage reduction in residual strength for the case where the lead crack tips just penetrated the crack-arresting stringers, and the distance between the first MSD and the tip of the lead crack is 1 in. Three different cases were analyzed, corresponding to situations where 1) there is one rivet hole, with cracks, ahead of a lead-crack tip; 2) there are three rivet holes with MSD cracks, ahead of a lead-crack tip; and 3) there are five rivet holes with MSD cracks ahead of a lead-crack tip. Figure 20 shows how the residual strength decreases as the size and the number of rivet-hole cracks increase. The more MSD cracks, the larger is the reduction in residual strength. Although the fatigue damage can significantly reduce the residual strength of the panel, the panel will not lose the capability to arrest a two-bay circumferential crack at the operating stress level (assumed to be 34 ksi) until the MSD cracks are of significant length. This can be seen in Fig. 21.

VI. Conclusions

A numerical study of the residual strength of an aircraft fuselage in the presence of MSD/MED has been carried out using a software package developed to facilitate automated analyses of full-scale fuselage panels with WFD, a hierarchical modeling approach, and an EPFEAM.

Numerical results show a significant reduction in residual strength due to the presence of MSD when elastic–plastic analyses are performed. Using the elastic–plastic assumption, the effects of the location of the two-bay crack on the residual strength have also been studied. In addition, the interaction of multiple cracks, including MSD cracks, with a two-bay crack has been studied.

A circumferential crack at a critical location in the fuselage with high axial stress is also analyzed. Very large plastic zones are observed, with a radius of more than 5 in. at the critical loads. Plastic deformation near rivet holes is also very significant. The effect of the yielding and failure of the rivets on the crack-arresting stringers is to decrease the crack-arresting capability of a circumferentially cracked fuselage, as do the multiple site damages in the skin of the fuselage. Because the LEFM approach significantly overestimates the residual strength of a cracked panel and underestimates the influence of MSD, the EPFM approach is mandatory for the study of residual strength of a circumferential crack at critical locations.

Thus, this paper shows the importance of EPFM in the assessment of the residual strength of a fuselage with longitudinal/circumferential lead cracks, with and without MSD. This paper also shows the strong interaction between multiple lead cracks.

Acknowledgments

The work of the first author was supported by a grant from the Federal Aviation Administration (FAA) to the University of California, Los Angeles (UCLA), as well as by the office of the Dean of the School of Engineering and Applied Science at UCLA. The support of the FAA Center of Excellence at Georgia Institute of Technology is also gratefully acknowledged.

References

[1]Atluri, S. N., *Structural Integrity and Durability*, Tech Science Press, 1997.

[2]Maclin, J. R., "Performance of Fuselage Pressure Structure," *International Conference on Aging Aircraft and Structural Airworthiness*, NASA CP 3160, 1991, pp. 67–74.

[3]Swift, T., "Widespread Fatigue Damage Monitoring—Issues and Concerns," *Proceedings of the 5th International Conference on Structural Airworthiness of New and Aging Aircraft*, Washington, DC, 1993, pp. 133–150.

[4]Jeong, D. Y., and Tong, P., "Threshold of Multiple Site Damage in Aging Airplanes," *Structural Integrity in Aging Aircraft*, ASME-AD Vol. 47, American Society of Mechanical Engineers, New York, 1995, pp. 63–71.

[5]Swift, T., "Effect of MSD on Large Damage Residual Strength," *Contemporary Research in Engineering Science*, edited by R. C. Batra, 1995, pp. 516–539.

[6]Wang, L., Brust, F. W., and Atluri, S. N., "The Elastic–Plastic Finite Element Alternating Method and the Prediction of Fracture Under WFD Conditions in Aircraft Structures," *Computational Mechanics*, Vol. 19, No. 5, 1997, pp. 356–369.

[7]Wang, L., Brust, F. W., and Atluri, S. N., "The Elastic–Plastic Finite Element Alternating Method (EPFEAM) and the Prediction of Fracture Under WFD Conditions in Aircraft Structures. Part II. Fracture and the T^*-Integral Parameter," *Computational Mechanics*, Vol. 19, No. 5, 1997, pp. 370–379.

[8]Wang, L., Brust, F. W., and Atluri, S. N., "The Elastic–Plastic Finite Element Alternating Method (EPFEAM) and the Prediction of Fracture Under WFD Conditions in Aircraft Structures. Part III. Computational Predictions of the NIST Multiple Site Damage Experimental Results," *Computational Mechanics*, Vol. 20, No. 3, 1997, pp. 199–212.

[9]Atluri, S. N., *Computational Methods in the Mechanics of Fracture*, North-Holland, Amsterdam; also translated into Russian, Mir, Moscow, 1986.

[10]Wang, L., and Atluri, S. N., "Recent Advances in the Alternating Method for Elastic and Inelastic Fracture Analyses," *Computational Methods in Applied Mechanical Engineering*, Vol. 137, No. 1, 1996, pp. 1–58.

[11]Swift, T., "Fracture Analysis of Stiffened Structures," *Damage Tolerance of Metallic Structures*, ASTM STP 842, American Society for Testing and Materials, 1984, pp. 69–107.

R. K. Kapania
Associate Editor